Enhanced long-range communication among large scale brain networks during the pre-microsaccadic period

Ying Gao and Huiguang He
Laboratory of Brain Atlas and Brain-inspired Intelligence
Institute of Automation, Chinese Academy of Sciences,
Beijing 100190, China
Email: ying.gao@ia.ac.cn, huiguang.he@ia.ac.cn

Bernhard A. Sabel
Institute of Medical Psychology
Medical Faculty, Otto-von-Guericke University of Magdeburg
Magdeburg 39106, Germany
Email: Bernhard.Sabel@med.ovgu.de

***Abstract*—Microsaccades play a critical role in vision. They facilitate visual processing within the receptive field congruent with the anticipated microsaccade direction, while inhibiting processing elsewhere. This might be controlled by an interaction between the attention network and the visual network. In this study, we quantified the large-scale brain network dynamics time-locked to microsaccades, and found that the global communication efficiencies of these large-scale brain networks were significantly enhanced during the pre-microsaccadic period. Specifically, in theta and beta bands, areas of the attention network send information toward areas of the visual network and the posterior part of the default mode network; in alpha band, areas of the visual network and the posterior part of the default mode network send information back to the front. Our findings suggest that the enhanced long-range communication contributes to the pre-microsaccadic modulation of visual perception. The top-down attention modulation in the theta band and the bottom-up feedback in the alpha band collaboratively support the selective modulation of visual perception before microsaccade onset. Because microsaccades are continuously causing rhythmic modulation of the large-scale brain network communication, they should be taken into consideration when interpreting any visual and cognitive task results.**

Keywords—microsaccade, pre-microsaccadic modulation of visual perception, large-scale network, network efficiency, partial transfer entropy

I. Introduction

Seeing is not a passive process, but an active one, in which eye movements played a critical role. The sensitivity of the retina gradually decreases from the center to the periphery, Therefore, saccadic eye movements are continuously performed, moving targets of interest onto the fovea centralis of the retina, to fixate and extract visual information. Even when we are trying to hold our eyes still, they never are. Fixational eye movements including microsaccades, drifts and tremors, are continuously produced [1]. Among them, microsaccades are the small, fast, and jerk-like eye movements, which are on the same continuum and share the same singular generator circuits with saccades [2].

While being tiny (~ 1 deg), microsaccades are not too tiny to care. They not only support normal vision by courteracting fading, maintaining fixation accuracy, facilitating high-acuity vision and serving as an optimal sampling strategy to acquire information in relative small visual fields [1], but they also modulate visual perception in close temporal proximity [3]. Microsaccades selectively facilitate the visual processing of closely preceeding stimuli within $\pm 45^\circ$ of the microsaccade angle, but impede the visual processing of stimuli outside this range [3]. Such pre-microsaccadic modulation of visual perception may involve attention distribution and modulation of the visual system.

Yet, the dynamics of the large-scale networks related to attention modulation and visual processing during the pre-microsaccadic period has not been studied.

Gao et al. [4] demonstrated that microsaccadic rhythm can interact with ongoing brain oscillations, inducing alpha-band spectral perturbation over occipital region, and alpha-band phase synchrony over occipital, central and frontal regions [4]. Phase synchrony has been utilized to explore the long-range functional connectivity between different brain regions [5]. These "functionally connected" discrete brain regions form large-scale brain networks with different functions, such as the attention network, the default mode network and the visual network. During visual tasks, the visual network is involved in the processing of visual stimuli; the attention network is involved in top-down modulation of attention allocation based on the stimuli's relevance to the task; the default mode network on the other hand, is often deactivated during most stimulus-driven tasks [6-8]. Considering microsaccades are continuously executed, causing rhythmic fronto-occipital phase synchrony, we hypothesize that they also have impacts on the dynamics of different large-scale brain networks.

To this end, we recorded 19 participants' dense array EEG and high-resolution eye-tracking data simultaneously during a

This work was supported by the National Natural Science Foundation of China [grant numbers 62301560, 62020106015], Beijing Nova Program [grant number 20230484460] and China Postdoctoral Science Foundation [grant number 2021M703490].

fixation task. By quantifying the microsaccade-related brain network dynamics, we aim to reveal the specific communication pattern of different large-scale brain networks during the pre-microsaccadic period.

II. Method

A. Participants, Stimuli and Procedure

19 healthy participants (18-75 yrs, mean ± S.D. 43.2 ± 18.0 yrs, 9 female) participated in this study. All subjects had normal or corrected to normal visual acuity (20/20) and no visual field deficits as checked by perimetry. Written informed consent was obtained from all participants according to the Declaration of Helsinki (International Committee of Medical Journal Editors, 1991) after the institutional review board approved the study protocol.

Participants were instructed to maintain fixation at a fixation dot on a gamma corrected monitor (EIZO, CG241W, resolution of 2560 × 1440), which was placed at 67 cm distance. The white fixation dot (size: 10 pixels, luminance: 90 cd/m2) was presented against grey background (luminance: 29 cd/m2) in 40 trials lasting 7 sec each. The inter-stimulus interval was 3 sec, during which participants could rest their eyes. All participants were tested individually in a silent, dimly lit room.

B. Data recording and analysis

Binocular eye movements were recorded during the fixation task using an EyeLink-1000 system (SR Research, Ontario, Canada) with a sampling rate of 500 Hz and a spatial resolution of 0.01 degree. Head position was stabilized with a chin and forehead rest during eye tracker calibration, validation and recording. Microsaccade detection was performed based on the algorithm proposed by Engbert and colleagues [9-10]. A microsaccade was defined by the following criteria: (i) the velocity exceeded six median-based standard deviations of the velocity distribution; (ii) the duration exceeds 12 msec; (iii) the inter-saccadic interval exceeded 50 msec, otherwise only the largest microsaccade would be kept. We collected different microsaccade features such as rate (microsaccade number divided by detection time window length), amplitude (the Euclidean distance between the start and end point of the movement), velocity (the peak velocity during one microsaccade), duration, binocular microsaccade percentage (the proportion of binocular microsaccades in all detected microsaccades), horizontal and vertical binocular disconjugacy indices [11].

During the fixation task, dense array EEG was simultaneously recorded with the eye movement data, using a HydroCell GSN 128-channel net and Net Amps 300 amplifier (EGI Inc., Eugene, Oregon, USA). Our recording used a sampling rate of 500 Hz, a 200 Hz anti-aliasing low pass filter, Cz as a reference (ground electrode between Cz and Pz), and was digitalized with 24-bit precision. Common trigger pulses were sent from the presentation computer to both eye tracking computer and EEG recording device for offline co-registration of eye movements and EEG. Continuous EEG signal was re-referenced to the linked mastoids, filtered with high-pass (1 Hz) FIR filter, low pass (100 Hz) FIR filter, and notch (50 Hz) FIR filter. Eye tracking data and EEG data were synchronized and the synchronization quality was checked manually. Out-of-range eye tracking and EEG data were removed when there was a blink or when the eyes were not focused on the fixation point centered in a 4° × 4° window.

Binocular microsaccades and fixations were inserted as events into the EEG data. Epochs locked to fixation onsets [0 s to 1s] were extracted to compare with epochs locked to microsaccade onsets [-0.5 s to 0.5s], baseline corrected [0.3 s to 0.5 s for fixation eopchs, and −0.2 s to 0 s for microsaccade epochs], and manually screened for artifacts and noisy channels. Independent component analysis (ICA) was performed to remove artifacts [12].

C. Brain functional connectivity network analysis

For source estimation, the forward model was calculated using the symmetric boundary element method (BEM) [13] and default MNI MRI template (Colin 27). The inverse model was estimated using the weighted Minimum Norm Estimate (wMNE) [14]. After estimating the activation time-courses at 15,002 vertices (an equilateral triangle in the tessellation of the cortical surface), 68 anatomical regions of interest (ROIs; 34 in each hemisphere) were generated based on the Desikan – Killiany atlas [15] and activity of a seed voxel of each area was used to calculate functional connectivity.

Time frequency decomposition was conducted on source-based EEG single trials with Morlet wavelet (EEGlab newtimef function). The window size was set as 250 data points (500 ms). The wavelet contained 3 cycles at the lowest frequency (6 Hz) and the number of cycles was increasing up to 10 cycles at highest frequency (30 Hz) and 25 frequency points linearly spaced between 6 Hz and 30 Hz were estimated. After decomposition, for every participant, condition, and ROI, we obtained a 3D matrix of 25 (frequency points) × 200 (time points) × 'number of trials' (which varied between participants). To evaluate the functional coupling, the imaginary part of coherence (iCoh) [16] was computed for each frequency and time points between all possible pairs of ROIs.

The ROIs for the attention network, the default mode network and the visual network were selected based on He and his colleagues' findings [17]. To measure the large-scale brain network characteristics, these full iCoh adjacency matrices were converted into sparse, undirected, weighted graphs, which were further analyzed with graph measures. The threshold was adjusted for each full adjacency matrix to make sure the density of each graph (defined as the proportion of existing edges out of all possible edges) equals 0.20. We evaluated the global efficiency and the local efficiency [18]. These two measures provide information of the communication efficiency in different large-scale brain networks. On a global scale, efficiency quantifies the exchange of information across the network, while the local efficiency quantifies a network's resistance to failure on a small scale.

In addition, in order to explore the pattern of information flow during the pre-microsaccadic period, we calculated partial transfer entropy (PTE) within the theta (5-7 Hz), alpha (8-12 Hz) and beta (15-29 Hz) bands to quantify the directed

connectivity among different brain ROIs. The PTE between the random variables *x, y*, *z* (a potential source that drives both x and y), and *w* is defined as *PTE(w,X,Y|Z) = H(w,X,Z) + H(X,Z,Y) - H(X,Z) - H(w,X,Z,Y)*, where H is the differential entropy and *w* is the future of *x* [19].

D. Statistical analysis

Permutation tests were utilized to compare global efficiency, local efficiency, and PTE between microsaccade and fixation conditions. The number of randomization was set as 2000. The FDR method was applied to correct for multiple comparisons, and the family-wise alpha level was set to 0.05. Corrected p values were reported.

III. RESULTS

A. Microsaccade features

All 19 participants completed 40 trials during the fixation task. Within each trial, fixation period were extracted for microsaccade detection. Fig. 1 displays the main sequences of microsaccades from 19 participants, showing typical relationship between saccadic eye movements' peak velocity and amplitude [20].

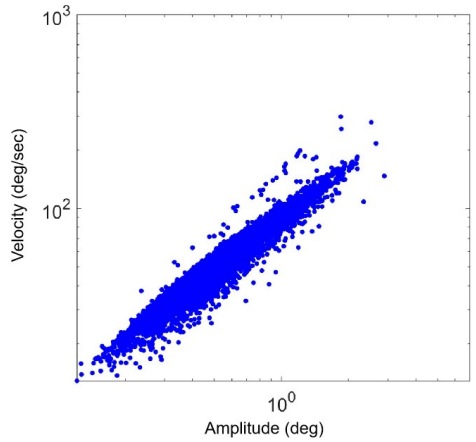

Fig. 1. Main sequences of microsaccades from 19 participants.

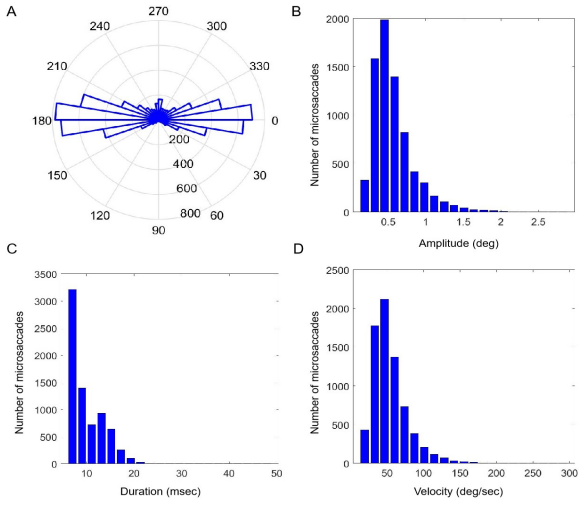

Fig. 2. Distributions of microsaccade features. A. Angular histogram of microsaccade direction. Bar length in the angular histograms represents microsaccade numbers. B. Histogram of microsaccade amplitude. C. Histogram of microsaccade duration. D. Histogram of microsaccade velocity.

During fixation, participants executed comparable number of microsaccades towards left or right, with microsaccade rate of 2.0 ± 0.6 Hz, microsaccades amplitude of 0.6 ± 0.3 deg; microsaccade velocity of 54.1 ± 24.4 deg/sec, and microsaccade duration of 10.3 ± 3.5 msec. Fig. 2 displays the angular histogram of microsaccade direction and histograms of microsaccade amplitude, duration and velocity.

Among the microsaccades executed, 44.2% ± 4.8% of them were binocular microsaccades, with horizontal disconjugacy of 6.1 ± 1.3 min arc and vertical disconjugacy of 7.5 ± 2.3 min arc. Fig. 3 displays the microsaccade binocular conjugacy pattern in one participant.

Fig. 3. Microsaccade binocular conjugacy pattern in one participant. The top

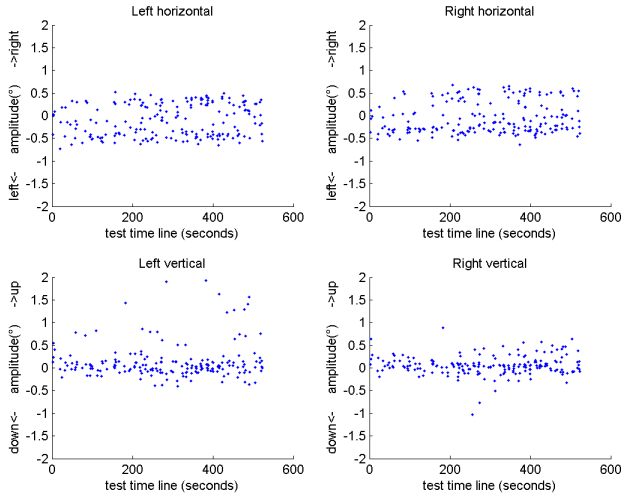

row displays the horizontal microsaccade component, while the bottom row displays the vertical microsaccade component. The left and right columns depict the movements of the left and right eyes, respectively.

B. Microsaccade-related global efficiency enhancement among large-scale brain networks

Compared to the fixation period, the peri-microsaccadic period exhibited enhancement of long-range communication within several large-scale brain networks.

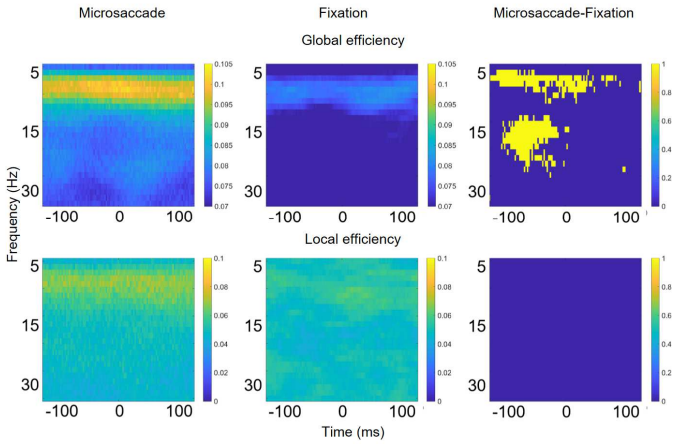

Fig. 4. Differences in local and global efficiency dynamics of the attention network between the peri-microsaccadic period and the fixation period. Only significant differences are illustrated in the third column.

The global efficiency of the attention network was significantly enhanced during the 100 ms before microsaccade onset, within the alpha band (tmass = 2883.8, p = 0.004) and the beta band (tmass = 5450.9, p = 0.004), while the local efficiency was comparable between the two conditions (Fig. 4).

As for the default mode network, the global efficiency was significantly enhanced from around 80 ms before to 80 ms after microsaccade onset, within the alpha (tmass = 2713.3, p = 0.003) and beta band (tmass = 5261.1, p = 0.003). The local efficiency was comparable between the two conditions (Fig. 5).

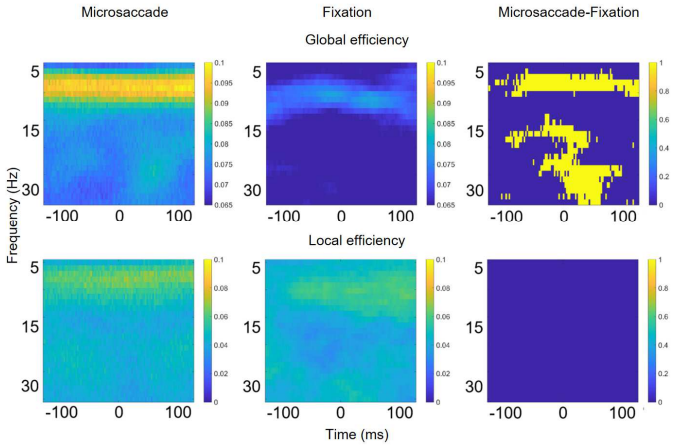

Fig. 5. Differences in local and global efficiency dynamics of the default mode network between the peri-microsaccadic period and the fixation period. Only significant differences are illustrated in the third column.

The global efficiency of the visual network was significantly enhanced from 100 ms before to around 90 ms after microsaccade onset within the alpha band (tmass = 2732.3, p = 0.003), and from around 30 ms before to around 80 ms after microsaccade onset within the beta band (tmass = 4362.2, p = 0.003), while the local efficiency was comparable between the two conditions (Fig. 6).

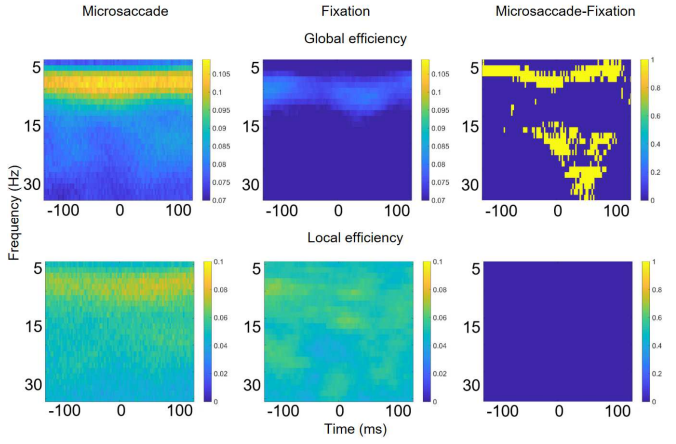

Fig. 6. Differences in local and global efficiency dynamics of the visual network between the peri-microsaccadic period and the fixation period. Only significant differences are illustrated in the third column.

C. *Pre-microsaccadic information flow among large-scale brain networks*

What's more, during the 100 ms before microsaccade onset, a specific information flow pattern was observed. Permutation tests revealed that the following directed functional connections were significantly stronger during the pre-microsaccadic period than the fixation period.

Within the theta band (Fig. 7), the left frontal pole sent information to both left and right caudal anterior cingulate cortex (t = 4.31, p = 0.002; t = 4.05, p = 0.002), and the left isthmus cingulate cortex (t = 4.36, p = 0.001); the left pars orbitalis sent information to the left transverse temporal cortex (t = 3.92, p = 0.002); and the right rostral anterior cingulate cortex sent information to the left pars triangularis (t = 4.15, p = 0.001). The main information flow was sent by the attention network towards the default mode network.

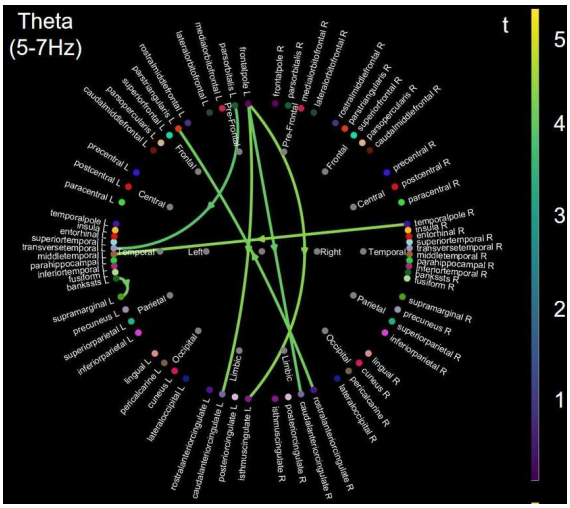

Fig. 7. Significantly stronger information flow within the theta band during the pre-microsaccadic period compared to the fixation period.

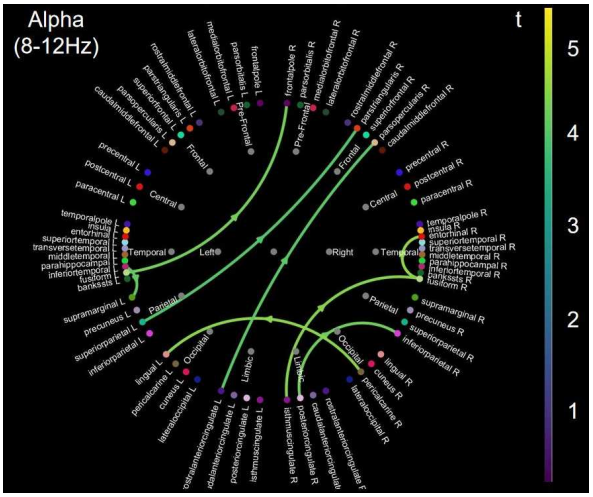

Fig. 8. Significantly stronger information flow within the alpha band during the pre-microsaccadic period compared to the fixation period.

Within the alpha band (Fig. 8), the right peri-calcarine region sent information to the left lingual gyrus (t = 4.38, p = 0.001) and the left inferior parietal cortex (t = 3.60, p = 0.001);

the left rostral anterior cingulate cortex sent information to the right pars opercularis (t = 3.96, p = 0.006); the right isthmus cingulate cortex sent information to the right fusiform gyrus (t = 4.33, p = 0.001); the left fusiform gyrus sent information to the right frontal pole (t = 4.19, p = 0.001); the right posterior cingulate cortex sent information to the right inferior parietal cortex (t = 4.15, p = 0.002); the left superior parietal cortex sent information to the right pars triangularis (t = 3.90, p = 0.002). The main information flow was sent by the default mode network and the visual network towards the attention network.

Within the beta band (Fig. 9), the left pars orbitalis sent information to the right peri-calcarine region (t = 4.44, p = 0.001). The main information flow was sent by the attention network towards the visual network.

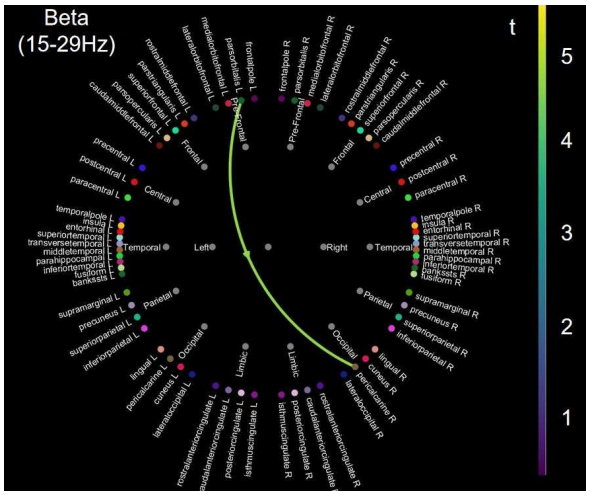

Fig. 9. Significantly stronger information flow within the beta band during the pre-microsaccadic period compared to the fixation period.

IV. Discussion and Conclusions

In this study, we measured the global and local efficiency dynamics of three large-scale brain networks during the pre-microsaccadic period and compared them to the fixation period. Our results showed that the global efficiencies of the attention network, default mode network and visual network were significantly enhanced around microsaccades (especially during the 100 ms before microsaccade onset) within the alpha and beta bands, while the local efficiencies of these large-scale brain networks were similar to those during fixation. These findings indicate that the long-range communication was enhanced before microsaccade onset, involving several large-scale brain networks. Furthermore, we analyzed the directed connection among the brain regions from different large-scale brain networks, and observed that bi-directional information transmissions were enhanced during the pre-microsaccadic period. Specifically, the frontal and pre-frontal regions, which belong to the attention network, send information toward the posterior brain regions, which belong to the visual network and the posterior part of the default mode network, through the theta and beta bands; while the posterior brain regions send information back to the frontal regions through the alpha band.

Hillebrand et al. [21] have highlighted the frequency-dependent nature of information flow within large-scale brain networks. The dominant pattern of information flow from the frontal lobe toward a more distributed network in the theta band represents control from higher association areas over lower-level, perceptual processes, and also over the default mode network, which is recognized as top-down signaling [22]. Meanwhile, the dominant pattern of information from the parietal and occipital areas toward the frontal areas in the alpha band represents bottom-up signaling, which could be a consequence of enhanced top-down signaling in the theta band [23]. These bi-directional information transmissions occur within the 100 ms before microsaccade onset, during which the selective modulation of visual perception takes place.

Based on our findings, we propose that the enhanced long-range communication efficiency within the large-scale brain networks contributes to the modulation of visual perception during the pre-microsaccadic period. The top-down attention modulation in the theta band, coupled with the bottom-up feedback in the alpha band, collaboratively facilitate visual processing within the receptive field congruent with the anticipated microsaccade direction, while inhibiting processing elsewhere. Because microsaccades are continuously executed during fixation, their rhythmic modulation of large-scale brain network communication should be taken into consideration when interpreting the brain functional network dynamics during any cognitive tasks.

Acknowledgment

This work was supported by the National Natural Science Foundation of China [grant numbers 62301560, 62020106015], Beijing Nova Program [grant number 20230484460] and China Postdoctoral Science Foundation [grant number 2021M703490)].

References

[1] S. Martinez-Conde, S. L. Macknik, and D. H. Hubel, “The role of fixational eye movements in visual perception,” Nat. Rev. Neurosci, vol. 5, pp. 229-240, March 2004.

[2] J. Otero-Millan, S. L. Macknik, R. E. Langston, and S. Martinez-Conde, “An oculomotor continuum from exploration to fixation,” Proc. Natl. Acad. Sci. U S A, vol. 110, pp. 6175-6180, March 2013.

[3] Z. M. Hafed, C. Chen, and X. Tian, “Vision, perception, and attention through the lens of microsaccades: mechanisms and implications,” Front. Sys. Neurosci, vol. 9: 167, December 2015.

[4] Y. Gao, C. Huber, and B. A. Sabel, “Stable microsaccades and microsaccade-induced global alpha band phase reset across the life span,” Invest. Ophthalmol. Vis. Sci, vol. 59, pp. 2032-2041, April 2018.

[5] G. Buzsáki and A. Draguhn, “Neuronal oscillations in cortical networks,” Science, vol. 304, pp. 1926-1929, June 2004.

[6] S. L. Bressler and V. Menon, “Large-Scale Brain Networks in Cognition: Emerging Methods and Principles, ” Trends Cogn. Sci, vol. 14, pp. 277-290, June 2010.

[7] P. Qin and G. Northoff, “How is our self related to midline regions and the default-mode network?,” Neuroimage, vol. 57, pp. 1221-1233, August 2011.

[8] R. Ptak, “The frontoparietal attention network of the human brain: action, saliency, and a priority map of the environment,” The Neuroscientist, vol. 18, pp. 502-515, October 2012.

[9] R. Engbert and R. Kliegl, “Microsaccades uncover the orientation of covert attention,” Vision Res, vol. 43, pp. 1035-1045, April 2003.

[10] R. Engbert, “Microsaccades: A microcosm for research on oculomotor control, attention, and visual perception,” Prog. Brain Res, vol. 154, pp. 177-192, January 2006.

[11] Y. Gao and B. A. Sabel, “Microsaccade dysfunction and adaptation in hemianopia after stroke,” Restor. Neurol. Neurosci, vol. 35, pp. 365-376, August 2017.

[12] A. J. Bell and T. J. Sejnowski, “An information-maximization approach to blind separation and blind deconvolution,” Neural Comput, vol. 7, pp. 1129-1159, November 1995.

[13] A. Gramfort, T. Papadopoulo, E. Olivi, and M. Clerc, “OpenMEEG: opensource software for quasistatic bioelectromagnetics,” Biomed. Eng. Online, vol. 9, pp. 45, September 2010.

[14] M. S. Hämäläinen and R. J. Ilmoniemi, “Interpreting magnetic fields of the brain: minimum norm estimates,” Med. Bio. Eng. Comput, vol. 32, pp. 35-42, 1994.

[15] R. S. Desikan, F. Ségonne, B. Fischl, B. T. Quinn, B. C. Dickerson, D. Blacker, R. L. Buckner, A. M. Dale, R. P. Maguire, and B. T. Hyman, “An automated labeling system for subdividing the human cerebral cortex on MRI scans into gyral based regions of interest,” Neuroimage, vol. 31, pp. 968-980, July 2006.

[16] G. Nolte, O. Bai, L. Wheaton, Z. Mari, S. Vorbach, and M. Hallett, “Identifying true brain interaction from EEG data using the imaginary part of coherency,” Clin. Neurophysiol, vol. 115, pp. 2292-2307, October 2004.

[17] Y. He, J. Wang, L. Wang, Z. J. Chen, C. Yan, H. Yang, H. Tang, C. Zhu, Q. Gong, Y. Zang, and A. C. Evans, “Uncovering intrinsic modular organization of spontaneous brain activity in humans,” PloS one, vol. 4, pp. e5226, April 2009.

[18] M. Rubinov and O. Sporns, “Complex network measures of brain connectivity: uses and interpretations,” Neuroimage, vol. 52, pp. 1059-1069, September 2010.

[19] R. Vicente, M. Wibral, M. Lindner, and G. Pipa, “Transfer entropy−a model-free measure of effective connectivity for the neurosciences,” J. Comput. Neurosci, vol. 30, pp. 45-67, February 2011.

[20] B. L. Zuber, L. Stark, and G. Cook, “Microsaccades and the velocity-amplitude relationship for saccadic eye movements,” Science, vol. 150, pp. 1459-1460, December 1965.

[21] A. Hillebrand, P. Tewarie, E. Van Dellen, M. Yu, E. W. S. Carbo, L. Douw, A. A. Gouw, E. C. W. van Straaten, and C. J. Stam, “Direction of information flow in large-scale resting-state networks is frequency-dependent,” Proc. Natl. Acad. Sci. U S A, vol. 113, pp. 3867-3872, April 2016.

[22] J. N. Frey, P. Ruhnau, N. Weisz, “Not so different after all: The same oscillatory processes support different types of attention,” Brain Res, vol. 1626, pp. 183-197, November 2015.

[23] A. M. Bastos, J. Vezoli, C. A. Bosman, J. Schoffelen, R. Oostenveld, J. R. Dowdall, P. De Weerd, H. Kennedy, and P. Fries, “Visual areas exert feedforward and feedback influences through distinct frequency channels,” Neuron, vol. 85, pp. 390-401, January 2015.